Check for updates

Water Science & Technology

IWA PUBLISHING

© 2023 The Authors

Water Science & Technology Vol 87 No 3, 598 doi: 10.2166/wst.2023.021

# Study on the ozonation degradation of methylene blue enhanced by microchannel and ultrasound

Huiyang Liu [a,b], Jianfeng Yu [a,b,*] and Xiangyu Liu [c]

[a] Jiangsu Key Laboratory of Advanced Food Manufacturing Equipment & Technology, Wuxi, Jiangsu Province 214122, China
[b] School of Mechanical Engineering, Jiangnan University, Wuxi, Jiangsu Province 214122, China
[c] Chengxian College, Southeast University, Nanjing, Jiangsu Province 210088, China
*Corresponding author. E-mail: yujf@jiangnan.edu.cn

HL, 0000-0002-4775-1042

## ABSTRACT

Azo dye-containing wastewater poses serious risks of environmental pollution because it is generally biologically toxic and resistant to conventional wastewater treatment methods. A novel degradation system integrating ozone, microchannel, and ultrasound was designed to effectively degrade azo dye-contaminated wastewater. The effects of discharge voltage of dielectric barrier discharge (DBD) reactor, liquid flow rate, microchannel width, ultrasonic power, initial pH, and reaction temperature on methylene blue (MB) decolorization were studied. A maximum MB decolorization efficiency of 92.7% was obtained in the ozone/microchannel/ultrasound ($O_3$/MC/US) system with 14 min of treatment. In addition, the 14-min decolorization efficiency and TOC removal efficiency obtained in $O_3$/MC/US system were increased by 12.6 and 6.5%, respectively, compared to those obtained in the pure $O_3$ system. Based on the results of scavenging experiments, the combined effects of microchannel and ultrasound were proved to improve the contribution rate of hydroxyl radicals, thus improving the decolorization efficiency. The present work clearly illustrates that ozonation degradation can be effectively enhanced by microchannel and ultrasound, and also provides a feasible method for the treatment of organic wastewater.

**Key words:** methylene blue, microchannel, ozonation degradation, ultrasound, wastewater

## HIGHLIGHTS

- Combined effects of microchannel and ultrasound on ozonation degradation were clearly observed.
- The 14-min decolorization efficiency of methylene blue reached 92.7%, which was increased by 12.6% due to the combination of microchannel and ultrasound.
- Ozonation degradation was enhanced by the combination effects of microchannel and ultrasound through the promotion of indirect ozonation process.

This is an Open Access article distributed under the terms of the Creative Commons Attribution Licence (CC BY 4.0), which permits copying, adaptation and redistribution, provided the original work is properly cited (http://creativecommons.org/licenses/by/4.0/).

Downloaded from http://iwaponline.com/wst/article-pdf/87/3/598/1172616/wst087030598.pdf
by guest

GRAPHICAL ABSTRACT

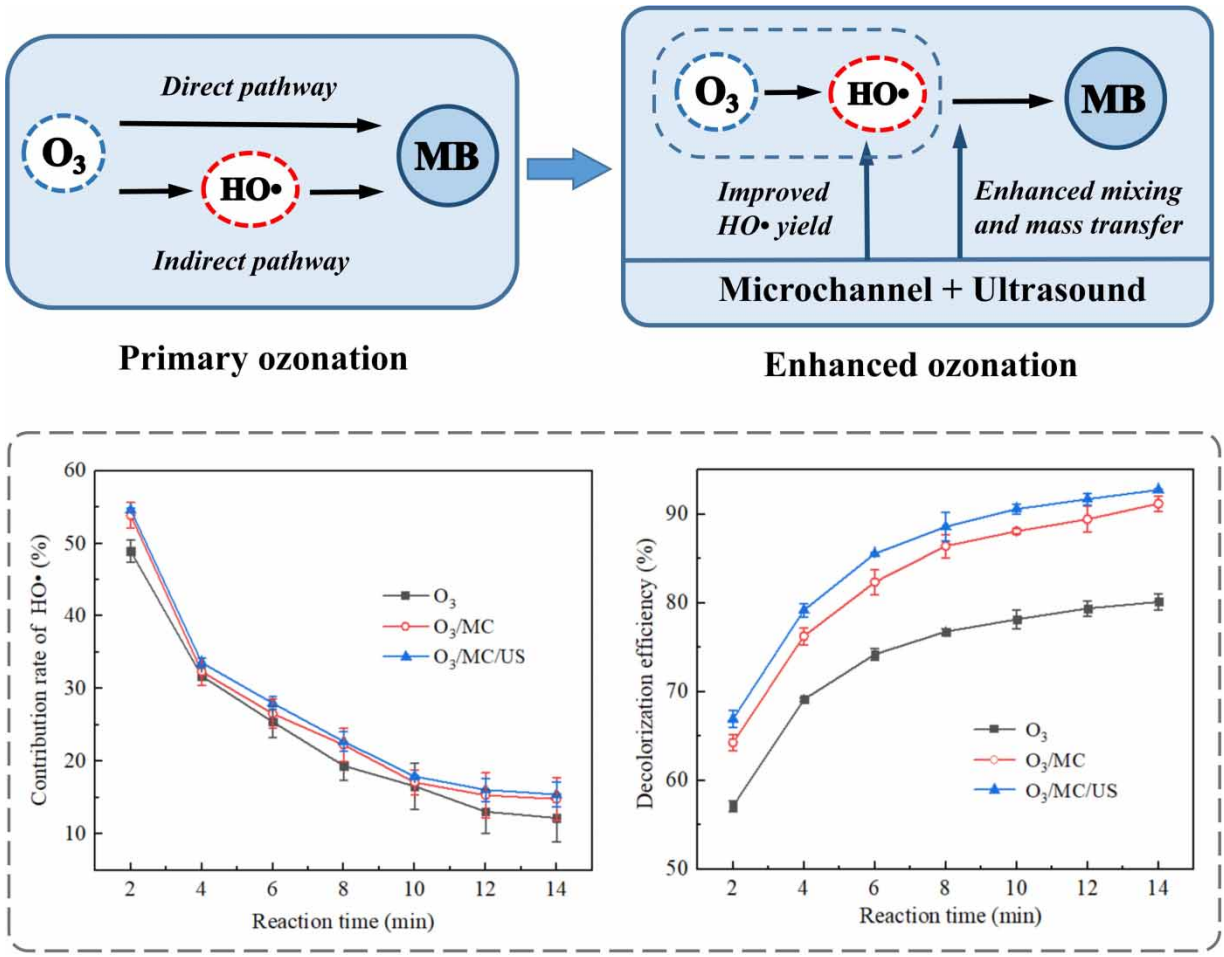


## 1. INTRODUCTION

Azo dyes are characterized by containing at least one azo group (–N = N–) bound to a chromophore or aromatic system (Sun *et al.* 2022). Due to the advantages of firm coloring and low production cost, azo dyes bring great convenience to our daily life. However, azo substances are generally toxic and non-biodegradable, and may cause serious water pollution even at low concentrations (Srivastava *et al.* 2022). Therefore, efficient degradation methods of azo-contaminated effluents are urgently needed to be investigated.

Unfortunately, conventional physical (Sun *et al.* 2006), chemical (Wu & Wang 2001) and biological (Prasac & Aikat 2014) treatment techniques are mineralized incomplete, time-consuming and uneconomical (Rayaroth *et al.* 2021). In recent years, advanced oxidation processes (AOPs) have been widely used for efficient and non-selective degradation of azo dyes (Bilińska & Gmurek 2021; Liu *et al.* 2021; Ismail & Sakai 2022). The principle of AOPs is to utilize the strong reactivity of hydroxyl radicals (HO•) to indiscriminately attack organic molecules, thus mineralizing the target pollutants (Dong *et al.* 2022). AOPs can be classified either as heterogeneous or homogeneous progress (Poyatos *et al.* 2010). Heterogeneous AOPs, referring to the processes using catalysts, have the advantages of environmental friendliness, high efficiency, and energy saving (Hou *et al.* 2022). Nevertheless, the difficulty of catalyst recovery limits the applications of heterogeneous AOPs in large-scale wastewater treatment. Homogeneous AOPs refer to the processes that use Fenton reagents (hydrogen peroxide with ferrous ions) and ozone ($O_3$) as the sources of HO•, with or without energy input. Although the Fenton process is widely used for its simplicity and efficiency, its major drawback is the production of iron sludge waste, which inevitably causes secondary pollution (Poyatos *et al.* 2010). Compared with other approaches, homogeneous AOPs based on ozonation have been considered a popular way due to their high oxidation potential and no generation of chemical byproducts (Zheng *et al.* 2022).

Downloaded from http://iwaponline.com/wst/article-pdf/87/3/598/1172616/wst087030598.pdf
by guest

$O_3$ is unstable in the aqueous medium and will spontaneously decompose through a complex mechanism involving HO• generation. Consequently, the ozonation degradation of azo dyes follows two pathways (Mehrjouei *et al.* 2015), including the direct pathway caused by molecular $O_3$ ($E^0(O_3/H_2O) = +2.07$ V), and the indirect pathway caused by HO• ($E^0(HO•/H_2O) = +2.8$ V). In the direct pathway, azo dyes are degraded by $O_3$ through oxidation–reduction reaction, cycloaddition reaction, electrophilic substitution reaction, and nucleophilic reaction (Issaka *et al.* 2021). In the indirect pathway, since HO• has a higher oxidation potential than $O_3$, and reacts with organic compounds $10^6$–$10^{12}$ times faster than $O_3$ (Munter 2001), azo dyes can be completely mineralized into carbon dioxide and water. The specific process of mineralization generally includes C–N bond rupturing, desulfurization reaction, and denitrification reaction (Shamsabadi & Behpour 2021). However, the use of ozonation treatment without any enhancement method is limited by low $O_3$ utilization (Miruka *et al.* 2021; Ghanbari *et al.* 2020) and poor HO• yield (Poyatos *et al.* 2010; Guo *et al.* 2015), because $O_3$ is difficult to dissolve and decompose spontaneously in aqueous solution (Wu *et al.* 2020). Therefore, the focus of this study is to investigate the possibility of the ozonation process enhanced by microchannel and ultrasound, as well as the resultant combination effects on MB degradation.

Microchannel can be used to improve $O_3$ utilization due to its large surface-to-volume ratio and short transport path. The ozonation degradation of azo dye Acid Red 14 enhanced by microchannel was reported to follow a pseudo-first-order kinetic model (Gao *et al.* 2012). The decolorization efficiency was observed to increase with the decrease of liquid volume flow rate in the microchannel. Additionally, the combination effect of microchannel on ozonation was investigated by MB degradation experiments with a microchannel reactor (Patinglag *et al.* 2019). It was found that the degradation efficiency was improved by a decreasing microchannel width in the range of 50–100 μm.

As another enhancement method, ultrasound can be used to improve the HO• yield and the mixing intensity of solutes. According to the hot-spot theory (Giray *et al.* 2018), the decomposition of $O_3$ into HO• will be promoted by the local excessive temperature released during the rupture of cavitation bubbles. The synergistic effect of ultrasound was investigated by combining a 520 kHz ultrasound with an ozonation process to degrade textile dyes (Tezcanli-Guyer & Ince 2004). The improvement of degradation efficiency was attributed to the enhancement of $O_3$ diffusion, electrophilic reaction, and radical reaction by ultrasound.

To the best of our knowledge, the combined applications of microchannel and ultrasound in the ozonation process are limited. In this study, we designed a novel degradation system that combines $O_3$, microchannel and ultrasound for the treatment of azo dye wastewater. The effects of the discharge voltage of DBD reactor, liquid flow rate, microchannel width, ultrasonic power, initial pH and reaction temperature on decolorization efficiency were studied. The combination effects of microchannel and ultrasound on ozonation degradation were clearly evaluated. The contribution of HO• to decolorization was also investigated by scavenging experiments. We, therefore, anticipated that this work would provide some theoretical and technical references for the treatment of azo dyes-containing effluents.

## 2. MATERIALS AND METHODS

### 2.1. Reagents

The target contaminant MB ($C_{16}H_{18}N_3ClS$) was purchased from the Tianjin Beilian Fine Chemicals Development Co., Ltd. Tertiary butanol (t-BuOH, $C_4H_{10}O$), sodium hydroxide (NaOH), and sulfuric acid ($H_2SO_4$) were obtained from Sinopharm Chemical Reagent Co. Ltd. All reagents used in this study were of analytical grade and used without further purification. Deionized water was used for the preparation of the required solutions. The solution pH was adjusted using 0.1 mM $H_2SO_4$ or NaOH.

### 2.2. Experimental apparatus and procedures

Figure 1 shows the structural diagram of the $O_3$/MC/US degradation system. $O_3$ was generated by a DBD reactor and released into the MB solution for the primary ozonation degradation. Subsequently, a part of the MB solution and $O_3$ gas were pumped into an ultrasonic microchannel reactor for enhanced ozonation degradation.

#### 2.2.1. $O_3$ generation

A DBD reactor (Jiangnan University, China) with a coaxial cylinder structure was used to continuously convert air into $O_3$ under room temperature and pressure. Two quartz glass tubes with a thickness of 2 mm and a length of 250 mm were used as the dielectric barriers, and their outer diameters were 40 and 48 mm, respectively. An air pump (Carmel Fluid Technology,

Downloaded from http://iwaponline.com/wst/article-pdf/87/3/598/1172616/wst087030598.pdf
by guest

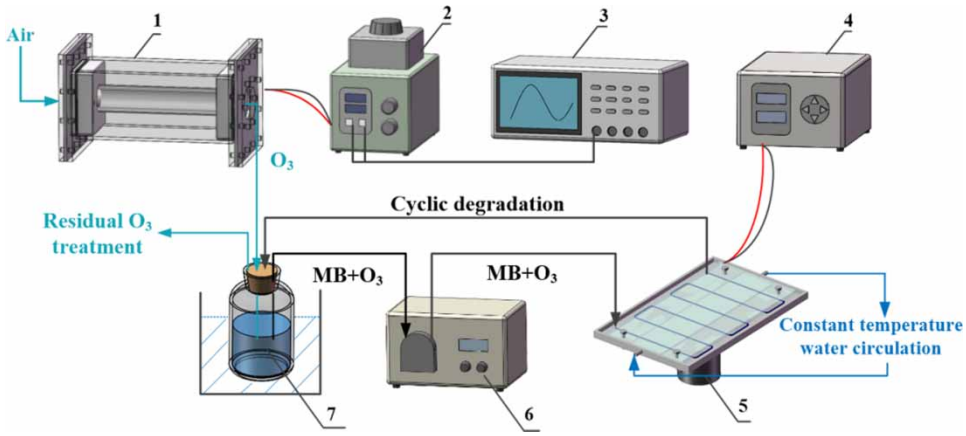


**Figure 1** | Structural diagram of the $O_3$/MC/US degradation system: (1) DBD reactor, (2) DBD power supply, (3) oscilloscope, (4) ultrasonic power supply, (5) ultrasonic microchannel reactor, (6) peristaltic pump, and (7) wide-mouth flask with constant temperature water bath.

China) was used to continuously feed air into the DBD reactor. A glass rotameter (Changzhou Shuanghuan, China) was used to control the inlet gas flow rate at 100 mL/min. A high-voltage power supply (CTP-2000K, Nanjing Suman Electronics, China) and a matching voltage regulator were used to apply an alternating voltage with a constant frequency of 6.8 kHz on the electrodes. The discharge voltage was measured by a voltage probe (P6015A, Tektronix, USA) and monitored by a digital oscilloscope (TBS2104B, Tektronix, USA). During the experiments, the DBD reactor was continuously air-cooled, and the residual $O_3$ was decomposed in water at a temperature of about 70 °C.

#### 2.2.2. Primary ozonation degradation

MB solutions with an initial concentration of 0.04 mM and varying pH values were configured using a precision electronic balance (Ningbo Yinzhou Huafeng, China) and a pH meter (Mettler Toledo Instrument, China). The primary ozonation degradation was carried out in a wide-mouth flask immersed in a constant temperature water bath. The $O_3$ gas was released into the MB solution through a silicone hose, whose outlet was fixed at 10 mm below the liquid level. A peristaltic pump (Carmel Fluid Technology, China) was used to pump $O_3$ gas and MB solution together into a microchannel through another silicone hose, whose inlet was fixed at 5 mm below the liquid level of the MB solution.

#### 2.2.3. Enhanced ozonation degradation

As shown in Figure 2, an ultrasonic microchannel reactor composed of an ultrasonic bath, cover plate, capillary, and ultrasonic oscillator was designed for the enhanced ozonation degradation. Three capillaries with inner diameters of 0.8, 1.0, and 1.2 mm were used as microchannels. The ultrasonic bath with a length, width, and depth of 200 mm × 125 mm × 6 mm was installed by bolt connection with the cover plate with a length, width, and thickness of 190 mm × 100 mm × 5 mm. Six parallel grooves were carved on the underside of the cover plate for inlay of capillaries. In addition, a groove with a length, width, and depth of 190 mm × 40 mm × 2.5 mm was carved on the underside of the cover plate. The constant temperature water could flow through the groove and directly contact with the capillaries to control the reaction temperature. An ultrasonic oscillator (Wuxi Hesen Technology, China) with a resonance frequency of 28 kHz was installed at the bottom of the ultrasonic bath. An ultrasonic power supply (Shenzhen Kemeida Ultrasonic Equipment, China) was used to drive the ultrasonic oscillator with a maximum power of 100 W.

### 2.3. Analytical methods

Percentage of color removal was used to analyze the progress of MB degradation. According to previous studies (Thangavadivel *et al.* 2014; Kodavatiganti *et al.* 2021), the decolorization efficiency, $\eta$, was defined as Equation (1).

$$\eta = \frac{Abs_0 - Abs_t}{Abs_0} \times 100\% \quad (1)$$

Downloaded from http://iwaponline.com/wst/article-pdf/87/3/598/1172616/wst087030598.pdf
by guest

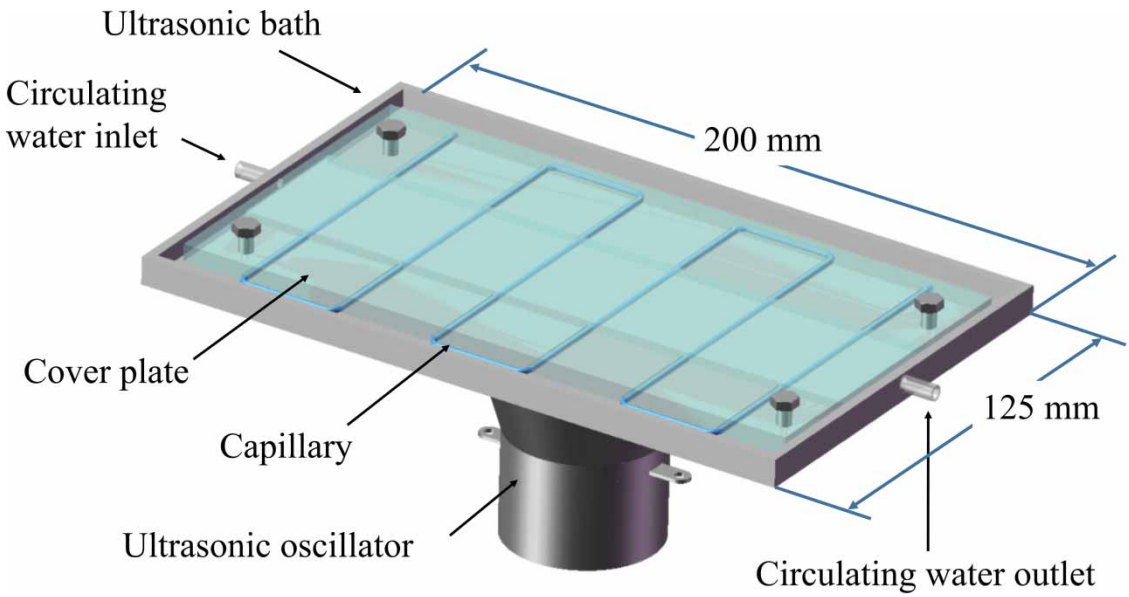


**Figure 2** | Diagram of the ultrasonic microchannel reactor.

where $Abs_0$ and $Abs_t$ represent the MB concentrations obtained by spectrophotometry before and after the decolorization, in mM. The absorbance of the MB solution was measured by an ultraviolet–visible spectrophotometer (Shimadzu, Japan). The absorbance calibration plot was initially obtained according to the spectrophotometric results of MB solutions with concentrations ranging from 0.005 to 0.05 mM. 3 mL of the decolorized MB solution was sampled for each measurement and tested at a maximum absorption wavelength of 664 nm.

The total organic carbon (TOC) was determined by an organic carbon analyzer (Shimadzu, Japan). The TOC removal efficiency, $E$, was calculated as Equation (2) (Can *et al.* 2019).

$$E = \frac{TOC_0 - TOC_t}{TOC_0} \times 100\% \tag{2}$$

where $TOC_0$ is the initial TOC concentration of MB solution, in mg/L. $TOC_t$ represents the TOC concentration of the degraded MB solution, in mg/L.

The percentage contribution of HO• to decolorization, $C$, was illustrated by Equation (3).

$$C = \frac{\eta_{total} - \eta_q}{\eta_{total}} \times 100\% \tag{3}$$

where $\eta_{total}$ and $\eta_q$ refer to the MB decolorization efficiency obtained without and with HO• quencher, respectively. With sufficient quencher addition, the MB decolorization will be dominated only by $O_3$ molecules, rather than by both $O_3$ and HO•. Consequently, the difference between $\eta_{total}$ and $\eta_q$ represents the decolorization efficiency contributed only by HO•.

### 2.4. Statistical analysis

To reduce the systematic error during the measurement, each test sample was measured by taking the average of two measurements. Origin software was employed for the statistical analysis of the experimental results. The goodness-of-fit of the absorbance calibration plot was evaluated based on the $R^2$ value (determination coefficient), where values less than 0.99 were considered statistically significant. Analysis of variance (ANOVA) was used to test the significance of the experimental results, and $p < 0.05$ was considered to be statistically significant.

Downloaded from http://iwaponline.com/wst/article-pdf/87/3/598/1172616/wst087030598.pdf
by guest

## 3. RESULTS AND DISCUSSION

### 3.1. Effect of discharge voltage of the DBD reactor

The discharge voltage of the DBD reactor affects the concentration of generated $O_3$. The $O_3$ generation can be improved by the increase of discharge voltage, while an excessive discharge voltage will cause a temperature rise, which may induce the decomposition of $O_3$ into oxygen. Therefore, it is significant to study the effect of discharge voltage on MB degradation. The initial pH was adjusted to 7, and the reaction temperature was controlled at 23 °C. According to Paschen's law (Eichhorn *et al.* 1993; Samaranayake *et al.* 2000), only when the discharge voltage is higher than 7.2 kV, the air between two electrodes will be broken down and converted into $O_3$. In the present work, the discharge voltage was adjusted by changing the regulating voltage. When the regulating voltages of 50, 60, and 70 V were applied, the corresponding discharge voltages measured by the oscilloscope were 7.8, 8.6, and 9.5 kV, respectively.

As shown in Figure 3, the MB decolorization efficiency increased with the increasing discharge voltage of the DBD reactor. When the discharge voltages were 7.8, 8.6, and 9.5 kV, the 14-min decolorization efficiency reached 71.0, 77.3, and 79.3%, respectively. The decolorization process was observed to follow first-order kinetics within 10 min, and the rate constants were 0.063, 0.065, and 0.081 $s^{-1}$ at discharge voltages of 67.8, 8.6, and 9.5 kV, respectively. The increase in discharge voltage can reduce the population density of low-energy electrons, which decompose the generated $O_3$, thereby improving the $O_3$ yield (Kitayama & Kuzumoto 1997). Statistical results have shown that the decolorization efficiency obtained at discharge voltages of 7.8 and 8.6 kV was statistically different within 14 min. When the discharge voltage was 9.5 kV, the decolorization efficiency obtained within 10 min was statistically different. However, under the continuous treatment at 9.5 kV discharge voltage for more than 10 min, the decolorization efficiency hardly increased with duration, and no statistical difference was observed. A reasonable reason is that the DBD reactor was overheated after operating for several minutes under the discharge voltage of 9.5 kV (Miruka *et al.* 2021). The overheating was caused by the energy consumption during discharge. It can be inferred that the high temperature destroyed the stability of $O_3$ gas, and also affected the discharge characteristics of the DBD reactor. In order to reduce the influence of $O_3$ decomposition caused by excessive temperature rise, the subsequent experiments were carried out at the discharge voltage of 8.6 kV. Furthermore, for the process of large-scale wastewater treatment, overheating of the reactors are needed to be avoided via adequate cooling or appropriate reduction of the discharge voltage.

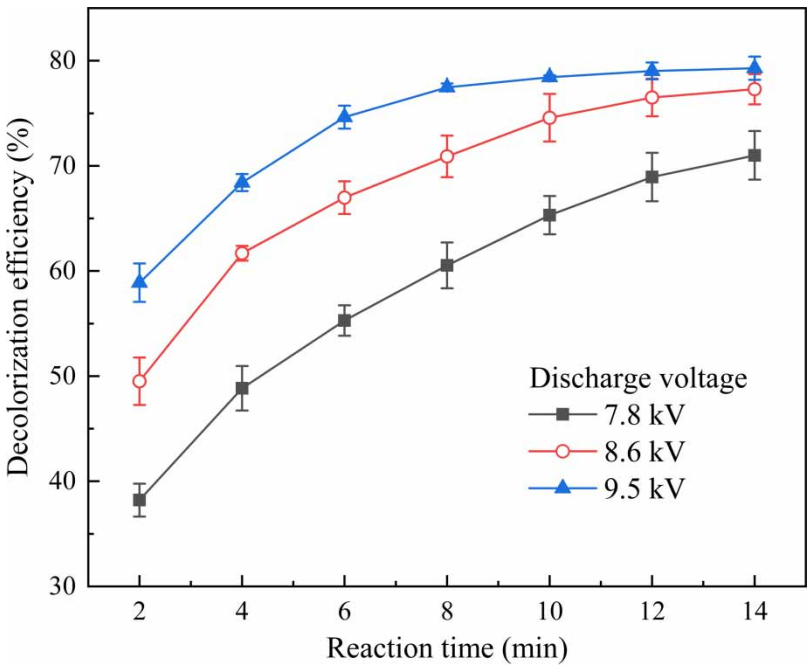


**Figure 3** | Effect of the discharge voltage of the DBD reactor on the MB decolorization efficiency in the $O_3$ system.

Downloaded from http://iwaponline.com/wst/article-pdf/87/3/598/1172616/wst087030598.pdf
by guest

### 3.2. Effect of liquid flow rate

The mixture of MB liquid flow and $O_3$ airflow was pumped into the microchannel reactor by a peristaltic pump. Since the MB liquid plugs were separated by $O_3$ gas pockets, a plunger flow was formed in the microchannel. The liquid flow rate of the MB solution can affect the length of the liquid plug, thus affecting the decolorization efficiency. As the liquid flow rate increases, the decolorization efficiency will therefore be improved as more MB solutions are involved in the degradation enhanced by microchannel. However, the increased liquid flow rate also led to a shorter residence time of the plunger flow in the microchannel, which could reduce the decolorization efficiency. Due to these two opposite effects on the decolorization efficiency, the effect of liquid flow rate was necessary to be studied. Experiments were conducted in $O_3$/MC system with the liquid flow rates ranging from 5 to 20 mL/min, the discharge voltage was 8.6 kV, the microchannel width was 1.2 mm, the initial pH was 7, and the reaction temperature was 23 °C. Reynolds (*Re*) numbers were used to analyse the dominant hydrodynamic conditions of microfluidics at varying liquid flow rates. The computed *Re* number increased from 5.6 to 22.4 when the liquid flow rate increased from 5 to 20 mL/min. These low *Re* numbers indicate that the prevailing flow was laminar, hence the mass transfer process was diffusion controlled. In addition, the actual *Re* numbers should be slightly higher than the calculated values, because the significant mixing effect of ultrasound changed the inertia and viscous force of the microfluidics in the microchannel.

As shown in Figure 4, the decolorization efficiency increased when the liquid flow rate increased from 5 to 15 mL/min. A maximum decolorization efficiency of 86.2% was obtained within 14 min at a liquid flow rate of 15 mL/min. Nevertheless, if the liquid flow rate was higher than 15 mL/min, there was a negative effect on the MB decolorization. Correspondingly, kinetic studies revealed that the first-order rate constants were 0.046, 0.054, 0.058, and 0.054 $s^{-1}$, when the liquid flow rates were 5, 10, 15, and 20 mL/min, respectively. The liquid flow rate affected both the specific surface area of the plunger flow and the residence time of the liquid slug in the microchannel. As the liquid flow rate increased from 5 to 15 mL/min, more MB solution entered the microchannel to involve in the enhanced ozonation degradation. Furthermore, the liquid convective effect in the microchannel was also intensified (Chaurasiya & Singh 2022), so the decolorization efficiency was increased. When the liquid flow rate increased from 15 to 20 mL/min, the liquid slugs of the plunger flow were excessively lengthened, thus reducing the gas–liquid mass transfer efficiency (Zhang *et al.* 2022). Additionally, the increasing liquid flow rate shortened the residence time of MB in microchannels, which also decreased the decolorization efficiency.

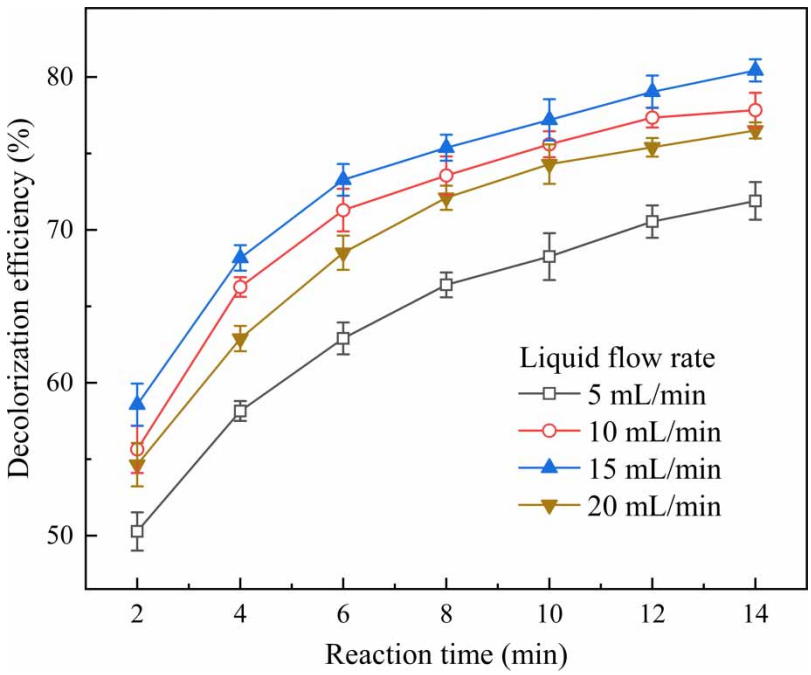


**Figure 4** | Effect of the liquid flow rate on the MB decolorization efficiency in the $O_3$/MC system.

Downloaded from http://iwaponline.com/wst/article-pdf/87/3/598/1172616/wst087030598.pdf
by guest

### 3.3. Effect of microchannel width

For a microchannel reactor, microchannel width is one of the important factors that affect the gas–liquid mass transfer efficiency, thus affecting the decolorization performance. The effects of microchannel widths ranging from 0.4 to 1.2 mm on MB decolorization were investigated. Experiments were carried out in $O_3$ and $O_3$/MC systems at initial pH of 7, reaction temperature of 23 °C, discharge voltage of 8.6 kV, and liquid flow rate of 15 mL/min. The *Re* numbers of the microfluids in the microchannels were 50.4, 33.6, 25.2, 20.2, and 16.8, when the inner diameters of the microchannels were 0.4, 0.6, 0.8, 1.0, and 1.2 mm, respectively.

As shown in Figure 5, by comparing the results obtained in $O_3$ and $O_3$/MC systems, a combined effect of microchannel on ozonation degradation was clearly observed. The decolorization efficiency increased first and then decreased with the increasing microchannel width. When the microchannel width was 0.4, 0.6, 0.8, 1.0, and 1.2 mm, the 14-min decolorization efficiency reached 79.7, 82.8, 86.2, 84.7, and 80.4%, respectively. Additionally, the corresponding rate constants determined by kinetic studies were 0.066, 0.072, 0.076, 0.072, and 0.058 $s^{-1}$, respectively. When the microchannel width increased from 0.4 to 0.8 mm, the 14-min decolorization efficiency increased from 79.7 to 86.2%. The improvement of decolorization efficiency can be attributed to the fact that the residence time of MB solution in the microchannel increased with the increase of microchannel width. Since the sufficient residence time ensured the contact time of MB solution and $O_3$ gas, the decolorization efficiency was improved. When the microchannel width increased from 0.8 to 1.2 mm, the 14-min decolorization efficiency decreased from 86.2 to 80.4%. Since the prevailing flow in the microchannel was laminar, the gas–liquid mass transfer process was largely realized by molecular diffusion. The reduction of the microchannel width meant a faster molecular diffusion rate (Bingham & Dunham 1997). Therefore, despite the decreasing microchannel width reducing the residence time of the MB solution in the microchannel, the MB decolorization efficiency was still improved due to the significant enhancement of the gas–liquid mass transfer.

### 3.4. Effect of ultrasonic power

Reasonable ultrasonic power helps in optimizing the operating cost for a given physicochemical transformation. Therefore, experiments were carried out in the $O_3$/MC/US system to study the effect of ultrasonic power on MB decolorization. The discharge voltage was 8.6 kV, the initial pH was 7, the reaction temperature was 23 °C, the liquid flow rate was 15 mL/min, the microchannel width was 0.8 mm, and the *Re* number of the liquid plug in the microchannel was 25.2.

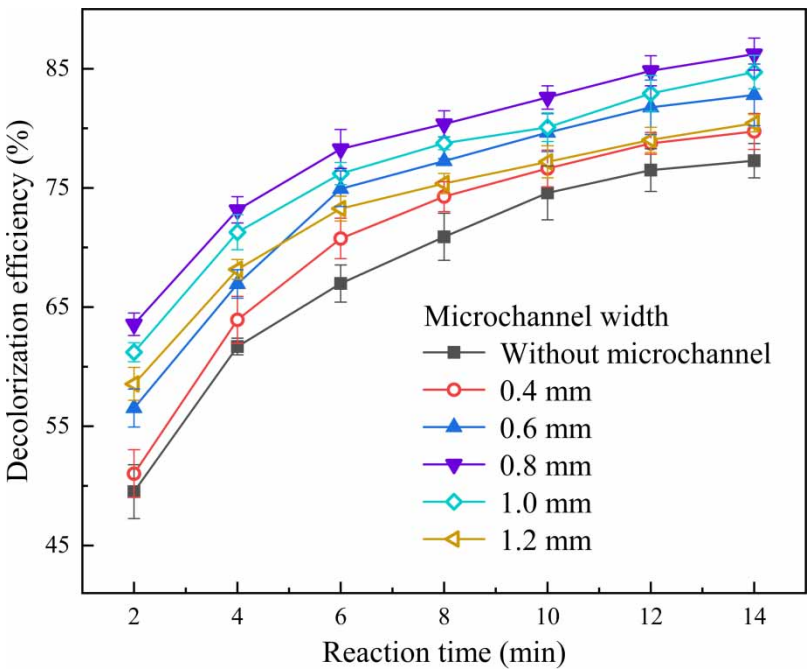


**Figure 5** | Effect of the microchannel width on the MB decolorization efficiency in $O_3$ and $O_3$/MC systems.

Downloaded from http://iwaponline.com/wst/article-pdf/87/3/598/1172616/wst087030598.pdf
by guest

As shown in Figure 6, the MB decolorization efficiency increased with the increase of ultrasonic power. The 14-min decolorization efficiency reached 86.6, 89.1, and 90.4%, with corresponding kinetic rate constants as 0.99, 1.01, and 1.06 $s^{-1}$, when the ultrasonic powers were 33, 66, and 100 W, respectively. The phenomenon that the application of ultrasound can promote decolorization is ascribed to the micromixing effect and thermal activation effect caused by acoustic streaming and acoustic cavitation, respectively (Ileri & Dogu 2022). With the increase of ultrasonic power, the reactions of $O_3$ decomposition into reactive species were promoted. The energized radicals initiated a series of chain reactions with $O_3$ to form extra free radicals (Chen *et al.* 2009). In the current experimental setup, the minimum power required for ultrasonic cavitation was about 33 W. Nonetheless, at high power levels (exceeded 66 W), the improvement of decolorization efficiency with the increase of ultrasonic power was not obvious. Excessive ultrasonic power resulted in bubble coalescence, bubble clustering, and acoustic impedance, thus reducing the cavitation effect. Thangavadivel *et al.* (2014) studied ultrasound-assisted decolorization of methyl orange in a microreactor. The results show that when the ultrasonic power was increased from 160 to 200 W, the decolorization efficiency was increased by less than 0.3%. The above observation by Thangavadivel *et al.* was consistent with Figure 6, which was also due to the obstruction of the cavitation process by excessive cavitation bubbles.

In addition, the ultrasonic oscillator was overheated after a long-time operation, which is common in the applications of ultrasonic devices. In this study, the temperature rise generated by ultrasound was controlled by a constant temperature water circulation. The temperature difference between the inlet and the outlet of the microchannel remained within 3–5 °C, which was low enough to avoid the interference of temperature rise on MB decolorization.

### 3.5. Effect of reaction temperature

Since the macroscopic rate constant of $O_3$ decomposition is a temperature dependent parameter (Miruka *et al.* 2021), the reaction temperature has a great influence on ozonation degradation. Therefore, the effect of reaction temperature was examined in the range of 23–60 °C. Experiments were carried out in $O_3$/MC/US system with a discharge voltage of 8.6 kV, initial pH of 7, a liquid flow rate of 15 mL/min, microchannel width of 0.8 mm, the *Re* number of 25.2, and ultrasonic power of 100 W. The temperature was maintained with a thermostatic bath that supplied circulating water to the wide-mouth flask and ultrasonic microchannel reactor.

As shown in Figure 7, the decolorization efficiency of MB decreased with an increasing reaction temperature. At the room temperature of 23 °C, the 14-min decolorization efficiency reached 90.4%, which was 2.2, 10.7, and 30% higher than that of

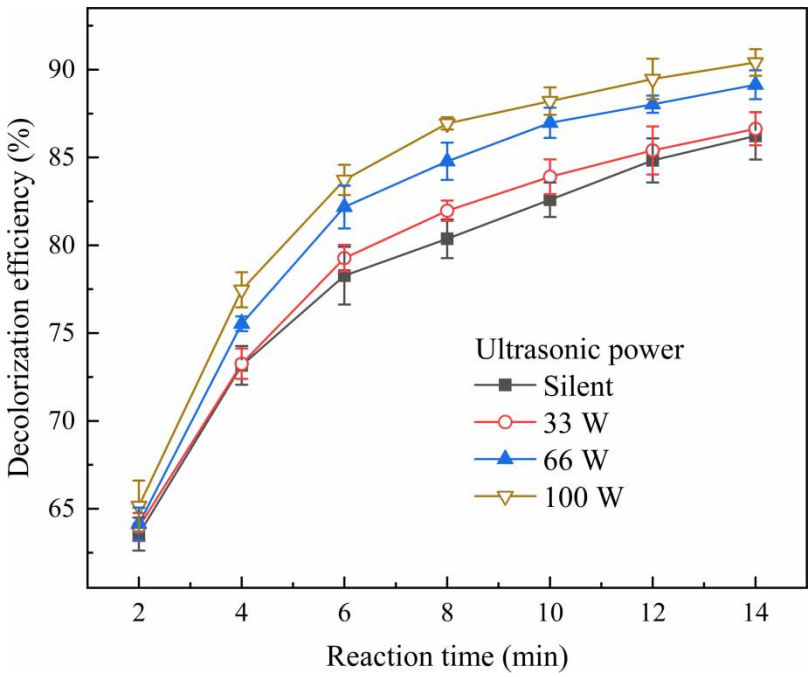


**Figure 6** | Effect of the ultrasonic power on the MB decolorization efficiency in the $O_3$/MC/US system.

Downloaded from http://iwaponline.com/wst/article-pdf/87/3/598/1172616/wst087030598.pdf
by guest

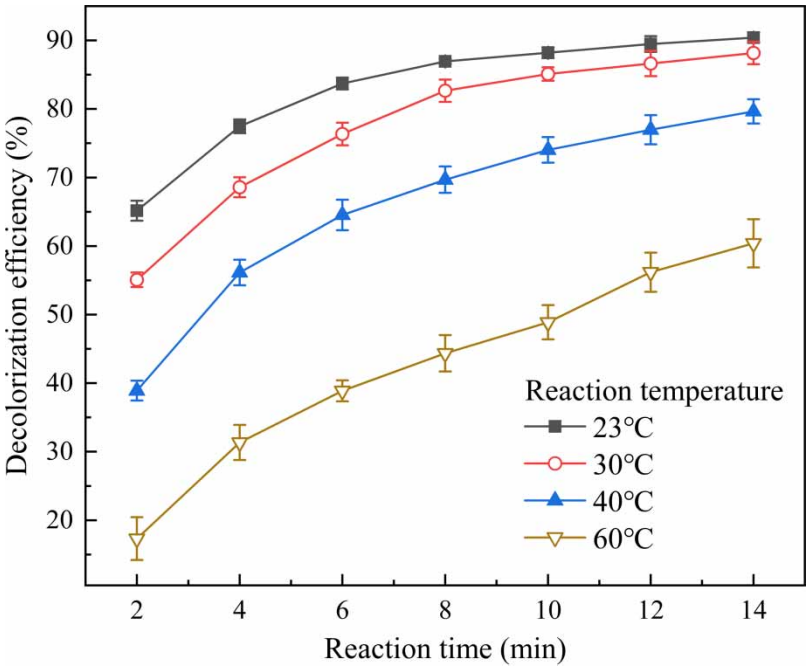


**Figure 7** | Effect of the reaction temperature on the MB decolorization efficiency in the $O_3$/MC/US system.

30, 40, and 60 °C, respectively. When the reaction temperature was 23, 30, 40, and 60 °C, the first-order rate constants of the decolorization were 1.06, 0.72, 0.44, and 0.11 $s^{-1}$, respectively. During the decolorization processes, the $O_3$ gas was released into the MB solution and stayed in the wide-mouth flask for several seconds. Since the spontaneous decomposition of $O_3$ into oxygen was promoted by the temperature rise, partial $O_3$ molecules could not complete the decolorization reactions before their lifetime achievements. In addition, the excessive temperature in the microchannel has been reported to hinder the mass transfer of gas molecules into the solutions (Lian *et al.* 2021), thus further reducing the decolorization efficiency.

### 3.6. Effect of initial pH

The pH of an aqueous solution can affect the number of oxides, the stability of reactive species, and the rate of chemical reactions during the ozonation process (Orhon *et al.* 2017). Therefore, the initial pH needs to be studied as a significant factor for ozonation degradation. It has been reported that when the pH value exceeds 11, excessive alkalinity has a scavenging effect on HO•. On the contrary, when the pH value is less than 5, the hydrolysis of $O_3$ is negligible (Kalmaz & Trieff 1986), and no longer dependent on pH. Based on the aforementioned studies, the effect of initial pH on MB decolorization was examined in the pH range of 3–11. The experiments were performed in the $O_3$/MC/US system with a reaction temperature of 23 °C, a discharge voltage of 8.6 kV, a liquid flow rate of 15 mL/min, a microchannel width of 0.8 mm, an *Re* number of 25.2, and an ultrasonic power of 100 W.

As shown in Figure 8, the decolorization was observed to conform to a first-order kinetic model, and the rate constants were 0.55, 0.78, 1.06, and 1.20 $s^{-1}$, when the initial pH values were 3, 5, 7, 9, and 11, respectively. Since the HO• yield was effectively increased by the increase of $HO^-$ dosage, the 14-min decolorization efficiency increased from 84.6 to 93.2% when the initial pH increased from 3 to 11. $O_3$ interacts selectively with organics in a molecular state under acidic or circumneutral pH. While under the alkaline conditions (Munter 2001), $O_3$ is easily hydrolyzed to produce highly reactive free radicals, mainly HO•. An obvious conversion of $O_3$ to HO• ($k = 2.2 \times 10^6\ M^{-1}s^{-1}$) was confirmed at a pH of 9 (Gunten 2003; Fajardo *et al.* 2013). $HO^-$ has been proven to be an initiator and promoter of $O_3$ hydrolysis, as described by Equations (4)–(9) (Hoigne & Bader 1983).

$$O_3 + HO^- \rightarrow HO_2^- + O_2 \quad (4)$$

$$HO_2^- + O_3 \rightarrow HO_2 \cdot + O_3^- \cdot \quad (5)$$

Downloaded from http://iwaponline.com/wst/article-pdf/87/3/598/1172616/wst087030598.pdf
by guest

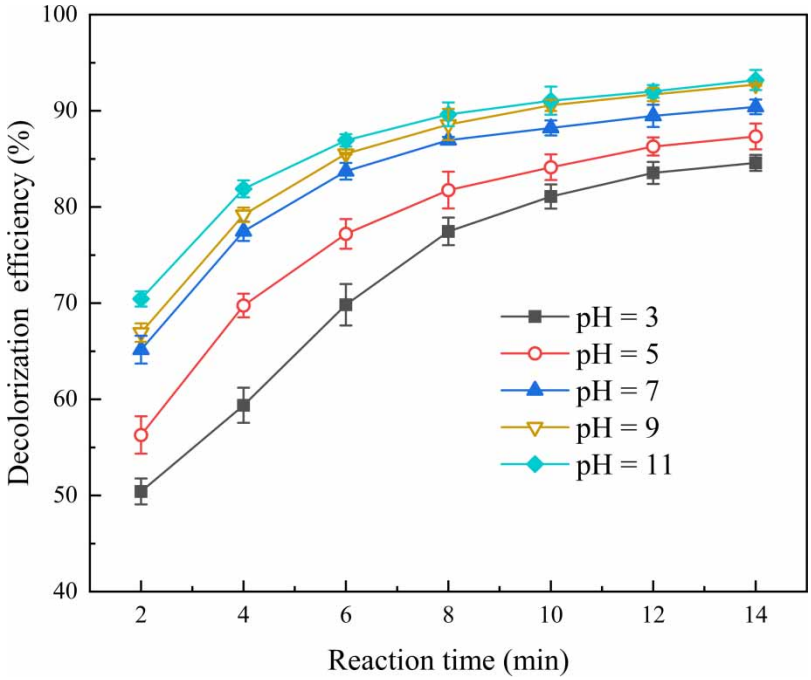


**Figure 8** | Effect of the initial pH on the MB decolorization efficiency in the $O_3$/MC/US system.

$$HO_2\cdot \rightleftharpoons H^+ + O_2^-\cdot \quad (6)$$

$$O_2^-\cdot + O_3 \rightarrow O_2 + O_3^-\cdot \quad (7)$$

$$O_3^-\cdot + H^+ \rightarrow HO_3\cdot \quad (8)$$

$$HO_3\cdot \rightarrow HO\cdot + O_2 \quad (9)$$

In addition, when the pH increased from 9 to 11, the 14-min decolorization efficiency increased from 92.7 to 93.2%. The slight improvement of the decolorization efficiency can be attributed to the gradual decrease in decolorization efficiency with the decrease of MB concentration (Zhang *et al.* 2013). Since a satisfactory efficiency can be obtained with a pH of both 9 and 11, an initial pH of 9 was chosen as a condition for subsequent experiments in consideration of saving reagents.

### 3.7. Combination effects of microchannel and ultrasound

Ultrasonic microchannel reactors have been successfully applied in liquid–liquid extraction (Thangavadivel *et al.* 2014) and Fenton degradation (John *et al.* 2016). The combination effects of microchannel and ultrasound in ozonation degradation were demonstrated, by comparing the MB decolorization efficiency obtained in $O_3$, $O_3$/MC, and $O_3$/MC/US systems. Experiments were carried out at a discharge voltage of 8.6 kV, microchannel width of 0.8 mm, a liquid flow rate of 15 mL/min, the *Re* number of 25.2, ultrasonic power of 100 W, reaction temperature of 23 °C, and an initial pH of 9.

As shown in Figure 9(a), kinetics studies showed that the first-order rate constants were 0.56, 0.11, and 0.12 $s^{-1}$ for the decolorization processed in $O_3$, $O_3$/MC, and $O_3$/MC/US systems, respectively. The 14-min decolorization efficiency obtained in the $O_3$/MC/US system was 92.7%, which was 12.6 and 2.4% higher than that in $O_3$ and $O_3$/MC systems. The decolorization performance observed in the $O_3$/MC/US system was better than that in both $O_3$ and $O_3$/MC systems. Consequently, the combination effects of microchannel and ultrasound on ozonation process have been clearly confirmed. In addition, the combination effect provided by microchannel was found to be more obvious than that provided by ultrasound.

The TOC removal was quantified to study the process of mineralization. As shown in Figure 9(b), the TOC removal was related to the decolorization process. For $O_3$, $O_3$/MC, and $O_3$/MC/US systems, the 7-min TOC removal efficiency was 49.5, 54.8, and 56.1%, respectively, as well as the 14-min TOC removal efficiency was 57.5, 62.1, and 64%, respectively.

Downloaded from http://iwaponline.com/wst/article-pdf/87/3/598/1172616/wst087030598.pdf
by guest

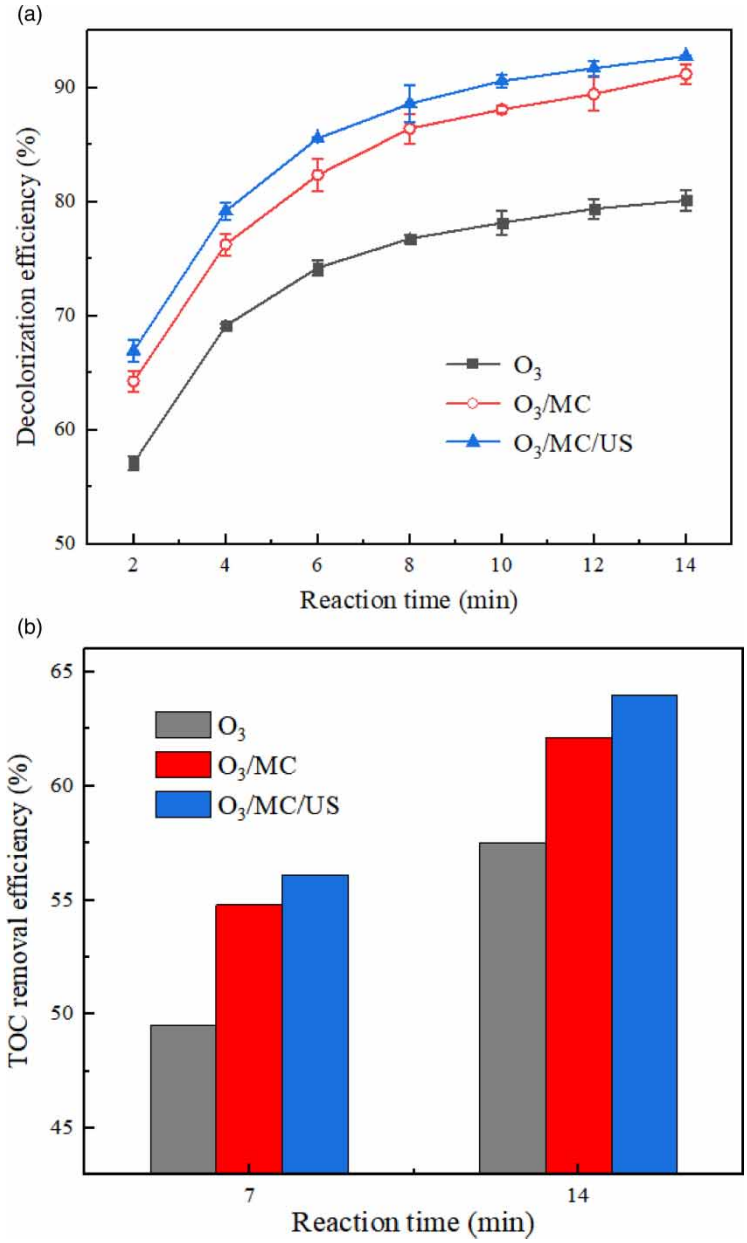


**Figure 9** | (a) Combination effects of microchannel and ultrasound on ozonation degradation. (b) TOC removal efficiency of $O_3$, $O_3$/MC, and $O_3$/MC/US systems.

Since part of the MB was degraded into organic intermediate compounds during ozonation, the TOC removal efficiency of each treatment method was lower than its decolorization efficiency. Anyhow, the TOC removal efficiency of both $O_3$/MC and $O_3$/MC/US treatments was higher than that of pure $O_3$ treatment, indicating that both microchannel and ultrasound can enhance the ozonation process.

### 3.8. Contribution rates of HO• in ozonation degradation

The roles of various reactive species involved in degradation processes can be elucidated by scavenging experiments. In this study, scavenging experiments were conducted to investigate the contribution rates of HO• in $O_3$, $O_3$/MC and $O_3$/MC/US systems. HO• was rapidly scavenged by t-BuOH ($3.8 \times 10^8$–$7.6 \times 10^8$ $M^{-1}s^{-1}$) (Miruka *et al.* 2021). The reaction temperature was 23 °C, initial pH was 9, discharge voltage was 8.6 kV, liquid flow rate was 15 mL/min, microchannel width was 0.8 mm, the corresponding *Re* number was 25.2, and ultrasonic power was 100 W.

Downloaded from http://iwaponline.com/wst/article-pdf/87/3/598/1172616/wst087030598.pdf
by guest

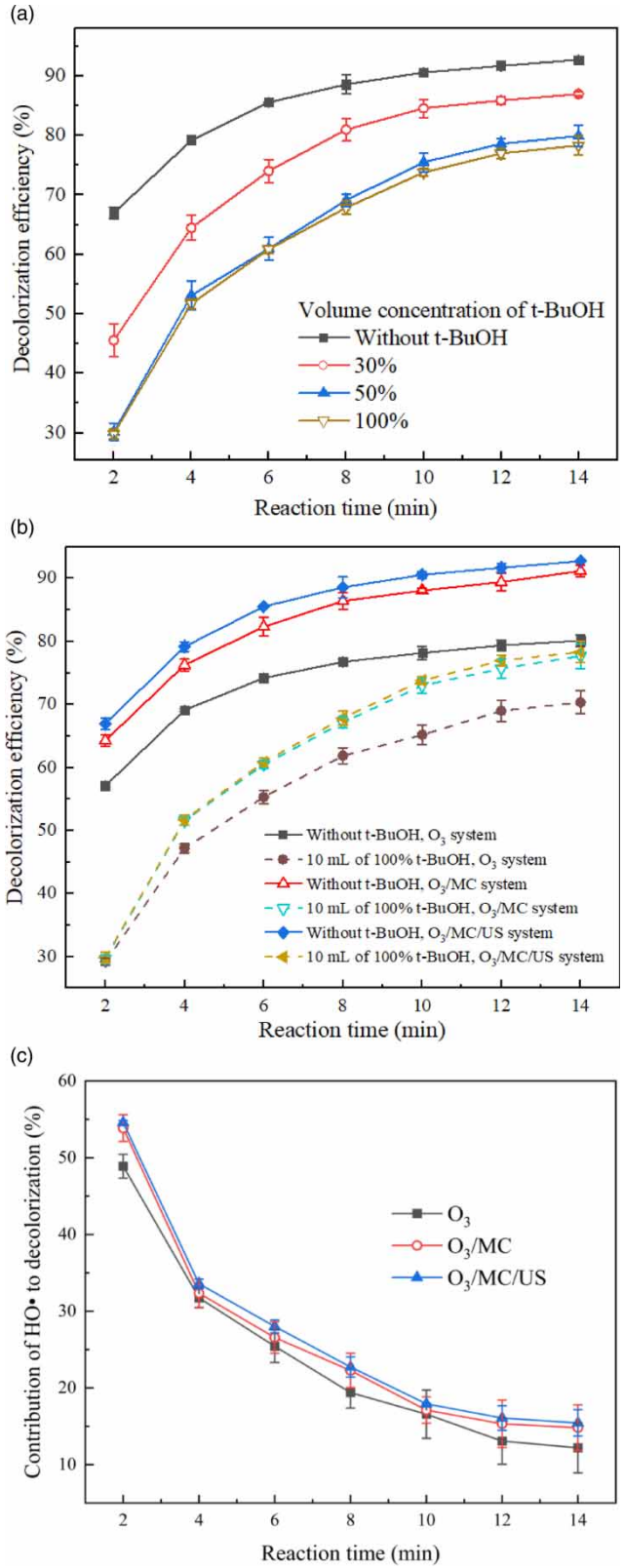


**Figure 10** | (a) Effect of the t-BuOH concentration on MB decolorization in the $O_3$/MC/US system. (b) Decolorization efficiency of MB with and without t-BuOH addition in $O_3$, $O_3$/MC, and $O_3$/MC/US systems. (c) Contribution of HO• to decolorization obtained by scavenging experiments in $O_3$, $O_3$/MC, and $O_3$/MC/US systems.

Downloaded from http://iwaponline.com/wst/article-pdf/87/3/598/1172616/wst087030598.pdf
by guest

As shown in Figure 10(a), in $O_3$/MC/US system, the addition of t-BuOH showed an obvious inhibition in MB decolorization. The 14-min decolorization efficiency was 86.9, 79.9, and 78.3% with the t-BuOH concentrations of 30, 50, and 100%, respectively. If the t-BuOH concentration was higher than 50%, the decolorization efficiency was almost no longer related to the t-BuOH dosage. A reasonable explanation is the indirect ozonation caused by HO• was largely inhibited, and only the direct ozonation caused by $O_3$ dominated the decolorization. The decolorization efficiency obtained with the inhibition of the radical scavenger was higher than that of some previous studies. This phenomenon can be attributed to the enhanced effect of microchannel and ultrasound on gas–liquid mass transfer. In $O_3$/MC/US system, the nucleophilic attack of $O_3$ was enhanced, so the decolorization efficiency can be maintained at a high level even after the HO• was quenched.

Figure 10(b) shows the time-courses of MB decolorization with and without t-BuOH addition in $O_3$, $O_3$/MC and $O_3$/MC/US systems. The complete scavenging of HO• reduced the 14-min decolorization efficiency by 9.8, 13.5, and 14.4% in $O_3$, $O_3$/MC, and $O_3$/MC/US systems, respectively. Based on these results, the contribution rates of HO• were calculated and shown in Figure 10(c). Qi *et al.* (2015) found that the 5-min and 15-min contribution rates of HO• reached about 18 and 11% in the catalytic ozonation of phenacetin. Figure 10(c) shows that in $O_3$ system, the 5-min and 14-min contribution rates of HO• reached about 26 and 12%, which were similar to the experimental results obtained by Qi *et al.* (2015). In addition, as the decolorization progressed from 2 to 14 min, the contribution rates of HO• decreased from about 50% to less than 20% in either system. As the decolorization proceeded, various small acidic molecules were produced as the intermediate products. The acidified solution hindered the HO• generation, thereby reducing the MB decolorization efficiency, which has been explained by Figure 8. Moreover, the contribution rates of HO• in $O_3$/MC/US system were higher than those in $O_3$/MC and $O_3$ system under the same experimental conditions. The 14-min contribution rates of HO• were about 15.5, 14.8, and 12.2% in $O_3$/MC/US, $O_3$/MC, and $O_3$ systems, respectively. As shown in Figure 10(b) and 10(c), the improvement rate on MB decolorization under the effect of ultrasound was not remarkably high. However, this is an observable trend, and could prove that ultrasound can enhance the ozonation process. During the experiments, the comprehensive effect of microchannel and ultrasound on the MB decolorization was existed. The MB decolorization efficiency was increased by 2.4% within 14 min due to the enhancement effect of ultrasound.

In addition, considering the complex chain reactions and interactions between reactive species, it was difficult to quantify all the contributors and precisely calculate their contributions. Therefore, the contribution rates obtained in this study were estimated values. Anyhow, the highest contribution rate of HO• was clearly observed in $O_3$/MC/US system. The combination effects of microchannel and ultrasound were confirmed to promote the indirect ozonation caused by HO•, thus increasing the MB decolorization efficiency.

## 4. CONCLUSIONS

MB was experimentally degraded in the newly designed degradation systems. The effects of discharge voltage, liquid flow rate, microchannel width, ultrasonic power, initial pH and reaction temperature on decolorization performance were investigated. The results show that the MB decolorization efficiency could be increased by an increasing discharge voltage, ultrasonic power, and initial pH, as well as a decreasing reaction temperature. The decolorization efficiency would be increased by an appropriate liquid flow rate, but would be decreased by both insufficient and excessive liquid flow rates. An increase of microchannel width in the proper range would be conducive to the color removal, otherwise, the excessive microchannel width would even cause a decrease in decolorization efficiency. For 100 mL MB solution with an initial concentration of 0.04 mM, a 14-min decolorization efficiency of 92.7% was obtained in the $O_3$/MC/US system, which was 12.6% higher than that in the pure $O_3$ system. In $O_3$/MC/US system, the 2-min and 14-min contribution rates of HO• reached 54.6 and 15.5%. In contrast, in pure $O_3$ system, the HO• contribution rates at 2 and 14 min were only 48.9 and 12.2%, respectively.

## ACKNOWLEDGEMENTS

The authors would like to thank Wuxi Hesen Technology Co., Ltd for providing ultrasonic oscillators and technical supports.

## FUNDING

This research did not receive any specific grant from funding agencies in the public, commercial, or not-for-profit sectors.

Downloaded from http://iwaponline.com/wst/article-pdf/87/3/598/1172616/wst087030598.pdf
by guest

## DECLARATION OF COMPETING INTEREST

The authors declare that they have no known competing financial interests or personal relationships that could have appeared to influence the work reported in this paper.

## DATA AVAILABILITY STATEMENT

All relevant data are included in the paper or its Supplementary Information.

## CONFLICT OF INTEREST

The authors declare there is no conflict.

## REFERENCES


Bilińska, L. & Gmurek, M. 2021 Novel trends in AOPs for textile wastewater treatment. enhanced dye by-products removal by catalytic and synergistic actions. *Water Resources and Industry* **26**, 100160. https://doi.org/10.1016/j.wri.2021.100160.

Bingham, N. H. & Dunham, B. 1997 Estimating diffusion coefficients from count data: Einstein-Smoluchowski theory revisited. *Annals of the Institute of Statistical Mathematics* **49** (4), 667–679. https://doi.org/10.1023/a:1003214209227.

Can, O. T., Gengec, E. & Koby, M. 2019 TOC and COD removal from instant coffee and coffee products production wastewater by chemical coagulation assisted electrooxidation. *Journal of Water Process Engineering* **28**, 28–35. https://doi.org/10.1016/j.jwpe.2019.01.002.

Chaurasiya, R. K. & Singh, K. K. 2022 CFD modelling of mass transfer in liquid-liquid core-annular flow in a microchannel. *Chemical Engineering Science* **249**, 117295. https://doi.org/10.1016/j.ces.2021.117295.

Chen, C., Lee, H., Chen, S., Chen, H. & Chang, M. 2009 Ultrasound-assisted plasma: a novel technique for inactivation of aquatic microorganisms. *Environmental Science & Technology* **43**, 4493–4497. https://doi.org/10.1021/es900345z.

Dong, C., Fang, W., Yi, Q. & Zhang, J. 2022 A comprehensive review on reactive oxygen species (ROS) in advanced oxidation processes (AOPs). *Chemosphere* **308** (1), 136205. https://doi.org/10.1016/j.chemosphere.2022.136205.

Eichhorn, H., Schoenbach, K. H. & Tessnow, T. 1993 Paschen's law for a hollow cathode discharge. *Applied Physics Letters* **63**, 2481–2483. https://doi.org/10.1063/1.110455.

Fajardo, A. S., Martins, R. C. & Quinta-Ferreira, R. M. 2013 Treatment of a simulated phenolic effluent by heterogeneous catalytic ozonation using $Pt/Al_2O_3$. *Environmental Technology* **34** (3), 301–311. https://doi.org/10.1080/09593330.2012.692720.

Gao, M., Zeng, Z., Sun, B., Zou, H., Chen, J. & Lei, S. 2012 Ozonation of azo dye acid red 14 in a microporous tube-in-tube microchannel reactor: decolorization and mechanism. *Chemosphere* **89**, 190–197. http://dx.doi.org/10.1016/j.chemosphere.2012.05.083.

Ghanbari, F., Khatebasreh, M., Mahdavianpour, M. & Lin, K. A. 2020 Oxidative removal of benzotriazole using peroxymonosulfate/ozone/ultrasound: synergy, optimization, degradation intermediates and utilizing for real wastewater. *Chemosphere* **244**, 125326. https://doi.org/10.1016/j.chemosphere.2019.125326.

Giray, S., Morcali, M. H., Akarsu, S., Ziba, C. A. & Dolaz, M. 2018 Comparison of classic fenton with ultrasound fenton processes on industrial textile wastewater. *Sustainable Environment Research* **28**, 165–170. https://doi.org/10.1016/j.serj.2018.02.001.

Gunten, U. V. 2003 Ozonation of drinking water: part II. Disinfection and by-product formation in presence of bromide, iodide or chlorine. *Water Research* **37**, 1469–1487. https://dio.org/10.1016/S0043-1354(02)00458-X.

Guo, W. Q., Yin, R. L., Zhou, X. J., Du, J. S., Cao, H. O., Yang, S. S. & Ren, N. Q. 2015 Sulfamethoxazole degradation by ultrasound/ozone oxidation process in water: kinetics, mechanisms, and pathways. *Ultrasonics Sonochemistry* **22**, 182–187. https://doi.org/10.1016/j.ultsonch.2014.07.008.

Hoigne, J. & Bader, H. 1983 Rate constants of reactions of ozone with organic and inorganic compounds in water II: dissociating organic compounds. *Water Research* **17**, 185–194. https://doi.org/10.1016/0043-1354(83)90099-4.

Hou, C., Li, Y., Niu, M., Liu, Y., Kong, X., Zhang, M. & Wang, L. 2022 Construction of an all-solid-state Z-scheme $Ag@Ag_3PO_4/TiO_2$-$(F_2)$ heterostructure with enhanced photocatalytic activity, photocorrosion resistance and mechanism insight. *Journal of Alloys and Compounds* **925**, 166765. https://doi.org/10.1016/j.jallcom.2022.166765.

Ileri, B. & Dogu, I. 2022 Sono-degradation of Reactive Blue 19 in aqueous solution and synthetic textile industry wastewater by nanoscale zero-valent aluminum. *Journal of Environmental Management* **303**, 114200. https://doi.org/10.1016/j.jenvman.2021.114200.

Ismail, G. A. & Sakai, H. 2022 Review on effect of different type of dyes on advanced oxidation processes (AOPs) for textile color removal. *Chemosphere* **291**, 132906. https://doi.org/10.1016/j.chemosphere.2021.132906.

Issaka, E., Amu-Darko, J. N. O., Yakubu, S., Fapohunda, F. O., Ali, N. & Bilal, M. 2021 Advanced catalytic ozonation for degradation of pharmaceutical pollutants – A review. *Chemosphere* **289**, 133208. https://doi.org/10.1016/j.chemosphere.2021.133208.

John, J. J., Kuhn, S., Braeken, L. & Gerven, T. V. 2016 Ultrasound assisted liquid-liquid extraction in microchannels – a direct contact method. *Chemical Engineering and Processing: Process Intensification* **102**, 37–46. https://dx.doi.org/10.1016/j.cep.2016.01.003.

Kalmaz, E. E. & Trieff, N. M. 1986 Kinetics of ozone decomposition and oxidation of a model organic compound in water. *Chemosphere* **15**, 183–194. https://dio.org/10.1016/0045-6535(86)90570-9.


Downloaded from http://iwaponline.com/wst/article-pdf/87/3/598/1172616/wst087030598.pdf
by guest

Kitayama, J. & Kuzumoto, M. 1997 Theoretical and experimental study on ozone generation characteristics of an oxygen-fed ozone generator in silent discharge. *Journal of Physics D-Applied Physics* **30**, 2453. https://doi.org/10.1088/0022-3727/30/17/011.

Kodavatiganti, S., Bhat, A. P. & Gogate, P. R. 2021 Intensified degradation of Acid Violet 7 dye using ultrasound combined with hydrogen peroxide, Fenton, and persulfate. *Separation and Purification Technology* **279**, 119673. https://doi.org/10.1016/j.seppur.2021.119673.

Lian, Z., Zhu, C., Zhang, S., Ma, W. & Zhong, Q. 2021 Study on the synergistic oxidation of sulfite solution by ozone and oxygen: kinetics and mechanism. *Chemical Engineering Science* **242**, 116745. https://doi.org/10.1016/j.ces.2021.116745.

Liu, L., Chen, Z., Zhang, J., Shan, D., Wu, Y., Bai, L. & Wang, B. 2021 Treatment of industrial dye wastewater and pharmaceutical residue wastewater by advanced oxidation processes and its combination with nanocatalysts: a review. *Journal of Water Process Engineering* **42**, 102122. https://doi.org/10.1016/j.jwpe.2021.102122.

Mehrjouei, M., Müller, S. & Mller, D. 2015 A review on photocatalytic ozonation used for the treatment of water and wastewater. *Chemical Engineering Journal* **263**, 209–219. https://doi.org/10.1016/j.cej.2014.10.112.

Miruka, A. C., Zhang, A., Wang, Q., Zhu, D., Wang, Z., Sun, Z., Heroux, P. & Liu, Y. 2021 Degradation of glucocorticoids in water by a synergistic system of peroxymonosulfate, microbubble and dielectric barrier discharges. *Journal of Water Process Engineering* **42**, 102175. https://doi.org/10.1016/j.jwpe.2021.102175.

Munter, R. 2001 Advanced oxidation processes – current status and prospects. *Proceedings of the Estonian Academy of Sciences* **32**, 91–101. https://doi.org/10.1002/chin.200141291.

Orhon, K. B., Orhon, A. K., Dilek, F. B. & Yetis, U. 2017 Triclosan removal from surface water by ozonation – kinetics and by-products formation. *Journal of Environmental Management* **204**, 327–336. https://dio.org/10.1016/j.jenvman.2017.09.025.

Patinglag, L., Sawtell, D., Iles, A., Melling, L. M. & Shaw, K. J. 2019 A microfuidic atmospheric-pressure plasma reactor for water treatment. *Plasma Chemistry and Plasma Processing* **39**, 561–575. https://doi.org/10.1007/s11090-019-09970-z.

Poyatos, J. M., Muñio, M. M., Almecija, M. C., Torres, J. C., Hontoria, E. & Osorio, F. 2010 Effectiveness of advanced oxidation processes in wastewater treatment: state of the art. *Water, Air, & Soil Pollution* **205**, 187–204. https://doi.org/10.3390/w13152094.

Prasac, S. S. & Aikat, K. 2014 Study of bio-degradation and bio-decolourization of azo dye by Enterobacter sp. SXCR. *Environmental Technology* **35**, 956–965. https://doi.org/10.1080/09593330.2013.856957.

Qi, F., Chu, W. & Xu, B. 2015 Ozonation of phenacetin in associated with a magnetic catalyst $CuFe_2O_4$: the reaction and transformation. *Chemical Engineering Journal* **262**, 552–562. https://doi.org/10.1016/j.cej.2014.09.068.

Rayaroth, M., Aravindakumar, C., Shah, C. & Boczka, G. 2021 Advanced oxidation processes (AOPs) based wastewater treatment – unexpected nitration side reactions – a serious environmental issue: a review. *Chemical Engineering Journal* **430**, 133002. https://doi.org/10.1016/j.cej.2021.133002.

Samaranayake, W., Miyahara, Y., Namihira, T., Katsuki, S., Hackam, R. & Akiyama, H. 2000 Ozone production using pulsed dielectric barrier discharge in oxygen. *IEEE Transactions on Dielectrics & Electrical Insulation* **7**, 849–854. https://doi.org/10.1109/94.891999.

Shamsabadi, K. & Behpour, M. 2021 Comparing photocatalytic activity consisting of $Sb_2S_3$ and $Ag_2S$ on the $TiO_2$-$SiO_2$/$TiO_2$ nanotube arrays-support for improved visible-light-induced photocatalytic degradation of a binary mixture of basic blue 41 and basic red 46 dyes. *International Journal Hydrogen Energy* **46**, 26989–27013. https://doi.org/10.1016/j.ijhydene.2021.05.199.

Srivastava, A., Rani, R. & Kumar, S. 2022 Optimization, kinetics, and thermodynamics aspects in the biodegradation of reactive black 5 (RB5) dye from textile wastewater using isolated bacterial strain, Bacillus albus DD1. *Water Science & Technology* **86** (3), 610. https://doi.org/10.2166/wst.2022.212.

Sun, J., Wang, X., Sun, J., Sun, R., Sun, S. & Qiao, L. 2006 Photocatalytic degradation and kinetics of Orange G using nano-sized Sn(IV)/$TiO_2$/AC photocatalyst. *Journal of Molecular Catalysis A: Chemical* **260**, 241–246. https://doi.org/10.1016/j.molcata.2006.07.033.

Sun, L., Mo, Y. & Zhang, L. 2022 A mini review on bio-electrochemical systems for the treatment of azo dye wastewater: state-of-the-art and future prospects. *Chemosphere* **294**, 133801. https://doi.org/10.1016/j.chemosphere.2022.133801.

Tezcanli-Guyer, G. & Ince, N. H. 2004 Individual and combined effects of ultrasound, ozone and UV irradiation: a case study with textile dyes. *Ultrasonics* **42**, 603–609. https://doi.org/10.1016/j.ultras.2004.01.096.

Thangavadivel, K., Konagaya, M., Okitsu, K. & Ashokkumar, M. 2014 Ultrasound-assisted degradation of methyl orange in a micro reactor. *Journal of Environmental Chemical Engineering* **2**, 1841–1845. https://dx.doi.org/10.1016/j.jece.2014.08.004.

Wu, J. & Wang, T. 2001 Ozonation of aqueous azo dye in a semi-batch reactor. *Water Research* **35**, 1093–1099. https://doi.org/10.1016/S0043-1354(00)00330-4.

Wu, Z., Abramova, A., Nikonov, R. & Cravotto, G. 2020 Sonozonation (sonication/ozonation) for the degradation of organic contaminants – A review. *Ultrasonics Sonochemistry* **68**, 105195. https://doi.org/10.1016/j.ultsonch.2020.105195.

Zhang, S., Wang, D., Zhang, S., Zhang, X. & Fan, P. 2013 Ozonation and carbon-assisted ozonation of methylene blue as model compound: effect of solution pH. *Procedia Environmental Sciences* **18**, 493–502. https://doi.org/10.1016/j.proenv.2013.04.066.

Zhang, Y., Zhu, C., Chu, C., Fu, T. & Ma, Y. 2022 Mass transfer and capture of carbon dioxide using amino acids sodium aqueous solution in microchannel. *Chemical Engineering and Processing: Process Intensification* **173**, 108831. https://doi.org/10.1016/j.cep.2022.108831.

Zheng, L., Zhang, J., Liu, X., Tian, L., Xiong, Z., Xiong, X., Chen, P., Wu, D. & Zou, J. 2022 Degradation of pesticide wastewater with simultaneous resource recovery via ozonation coupled with anaerobic biochemical technology. *Chemosphere* **300**, 134520. https://doi.org/10.1016/j.chemosphere.2022.134520.

First received 14 September 2022; accepted in revised form 14 January 2023. Available online 24 January 2023

Downloaded from http://iwaponline.com/wst/article-pdf/87/3/598/1172616/wst087030598.pdf
by guest